Davidson J., Wadhwa M., Hervig R., and Stephant A. (2020) Water on Mars: Insights from apatite in regolith breccia Northwest Africa 7034. *Earth and Planetary Science Letters* **552**, 116597.

Water on Mars: Insights from apatite in regolith breccia Northwest Africa 7034

Jemma Davidson[1,2]*, Meenakshi Wadhwa[2], Richard L. Hervig[2], Alice Stephant[1,2†]

[1]Center for Meteorite Studies, Arizona State University, 781 East Terrace Road, Tempe, AZ 85287-6004, USA.

[2]School of Earth and Space Exploration, Arizona State University, 781 East Terrace Road, Tempe, AZ 85287-6004, USA.

[†]Present address: Istituto di Astrofisica e Planetologia Spaziali -INAF, 00111 Roma, Italy

*Corresponding author: jdavidson@asu.edu

Earth and Planetary Science Letters
Volume 552, 15 December 2020, 116597

Cite as:

Davidson J., Wadhwa M., Hervig R., and Stephant A. (2020) Water on Mars: Insights from apatite in regolith breccia Northwest Africa 7034. *Earth and Planetary Science Letters* **552**, 116597.

https://doi.org/10.1016/j.epsl.2020.116597

Davidson J., Wadhwa M., Hervig R., and Stephant A. (2020) Water on Mars: Insights from apatite in regolith breccia Northwest Africa 7034. *Earth and Planetary Science Letters* **552**, 116597.

Abstract

Determining the source of planetary water from the hydrogen isotope compositions of crustal samples is complicated by the overprinting of isotopically diverse source material by geologic and atmospheric processes. As Mars has no plate tectonics, crustal material, which may have isotopically exchanged with the martian atmosphere, is not recycled into the mantle keeping the water reservoirs in the mantle and atmosphere mostly isolated, buffered by the crust. As the only known martian samples that are regolith breccias with a composition representative of the average crust of Mars, Northwest Africa (NWA) 7034 and its paired stones provide an important opportunity to investigate the water content and hydrogen isotope composition of the martian crust. In particular, apatites in distinct clasts as well as the brecciated matrix of NWA 7034 record a complex history including magmatic and impact processes, and exchange with crustal fluids.

Keywords: NWA 7034; regolith breccia; apatite; H-isotopes; martian crust; crustal fluid exchange

Davidson J., Wadhwa M., Hervig R., and Stephant A. (2020) Water on Mars: Insights from apatite in regolith breccia Northwest Africa 7034. *Earth and Planetary Science Letters* **552**, 116597.

1. Introduction

The total abundance and isotopic composition of hydrogen in crustal samples can yield insights into the origin and delivery mechanism(s) of water in planetary bodies in the inner Solar System. Water in the terrestrial planets may have been inherited from the protosolar nebula or delivered by carbonaceous chondrites and/or comets (see Hallis, 2017 and references therein). While Earth's primordial water has mostly been modified by processing within and between mantle and surface reservoirs driven largely by plate tectonics, Mars has not been tectonically active through much of its geologic history and its crustal material is not recycled, effectively isolating Mars' mantle and atmospheric H-bearing reservoirs. Thus, the H-isotope systematics of primary hydrous igneous minerals in martian meteorites may represent the H-isotope composition of Mars' water at the time that the rocks crystallized. However, determining the original, primordial water concentrations and H-isotopic compositions of the martian mantle is complicated by overprinting of various secondary processes. The measured H-isotopic systematics of hydrous, H-bearing minerals could have been affected by a number of geological and atmospheric processes such as fractionation during magmatic degassing, exchange with crustal fluids and/or the martian atmosphere, post-crystallization shock processing, and terrestrial weathering (Hallis, 2017 and references therein). Hydrogen isotopic compositions have been determined for various hydrous mineral phases from a number of martian meteorites including several shergottites, nakhlites, and chassignites as well as the ancient orthopyroxenite Allan Hills (ALH) 84001 (e.g., Watson et al., 1994; Leshin, 2000; Boctor et al., 2003; Greenwood et al., 2008; Hallis et al., 2012; Hu et al., 2014). These samples are not considered representative of the bulk of the martian crust (e.g., McSween et al., 2009; Agee et al., 2013) and have experienced varying degrees of impact-related shock (~5 to 55 GPa; Fritz et al., 2005). Of the ~120 known martian meteorites, only Northwest Africa (NWA) 7034 and its paired samples chemically match the composition of the martian crust determined by spacecraft missions (both the orbiting gamma-ray spectrometer onboard Mars Odyssey and the Mars rovers; Agee et al., 2013; Cannon et al., 2015). Moreover, the NWA 7034 pairing group has experienced low shock (5 to 15 GPa; Wittmann et al., 2015) and has the highest bulk water contents of all known martian meteorites (~6000 ppm; Agee et al., 2013), an order of magnitude (or more) higher than any of the other known martian meteorites. Therefore, NWA 7034 could provide key insights into water in the martian mantle and the crust, and the evolution of water reservoirs on Mars.

The NWA 7034 martian meteorite is a polymict regolith breccia of bulk basaltic composition, composed of a variety of mineral fragments and clasts of igneous, sedimentary, and impact origin (Fig. A1; e.g., Agee et al., 2013; Santos et al., 2015). Since it was recognized to be of martian origin, ~17 paired samples have been identified, including NWA 7475 (e.g., Wittmann et al., 2015), NWA 7533 (e.g., Humayun et al., 2013; Beck et al., 2015), and NWA 11522 (e.g., Smith et al., 2019). These paired samples differ from the other known martian meteorites not only in their petrology (the polymict breccia contains lithologies previously unrepresented in the martian meteorites; Santos et al., 2015), but also in some other significant characteristics. In particular, while most of the other known martian meteorites are <1.3 Ga, the zircon-bearing source lithologies of the NWA 7034 polymict breccia have an ancient age of >4.3 Ga (Humayun et al., 2013;

McCubbin et al., 2016a; Cassata et al., 2018). Also, NWA 7034 has a somewhat heavier oxygen isotope composition in $\delta^{17}O$, $\delta^{18}O$ and $\Delta^{17}O$ (Agee et al., 2013) compared to other known martian meteorites. As such, NWA 7034 and its paired samples represent unique crustal materials for investigating mantle processes and constraining the composition of the crust on Mars.

The crystallization age of the NWA 7034 source lithologies is estimated to be 4420 ± 70 Ma (Cassata et al., 2018), in agreement with the radiogenic dating of zircons in NWA 7034 and NWA 7533 (Humayun et al., 2013; McCubbin et al., 2016a). Therefore, the NWA 7034 source lithologies are the oldest among the martian meteorites, even older than the ancient martian orthopyroxenite ALH 84001 with an age of 4092 ± 30 Ma (Lapen et al., 2010). A Sm–Nd isochron age of ~4.4 billion years determined from matrix minerals and igneous clasts within NWA 7034 suggests contemporaneous formation of the breccia's various lithological components (Nyquist et al., 2016). However, NWA 7034 and its paired stones have not remained unaltered since formation; the U–Pb systematics of apatites and metamict zircons were reset at ~1.5 Ga by a single pervasive thermal event at a temperature of 500–800°C (McCubbin et al., 2016a; Hu et al., 2019). This event has been interpreted by McCubbin et al. (2016a) to be the result of impact processing, at which point brecciation and lithification took place. Alternatively, based on K–Ar systematics, it was suggested that this event marks the beginning of several hundred million years of thermal metamorphism consistent with plume magmatism, followed by ~1 Ga of inactivity until another event recorded by U-Th-Sm/He systematics, possibly brecciation, occurred at ~110 Ma (Cassata et al., 2018). It remains unclear whether these breccias were produced by volcanic (pyroclastic) activity, impacts, or a combination of both, although impacts are favored (McCubbin et al., 2016a). While there is clear evidence for the presence of impact-produced material in this regolith breccia, the impact events were not sufficiently energetic to generate high-pressure phases such as ringwoodite, bridgmanite, maskelynite, or glassy matrix (Santos et al., 2015). Although the high-pressure phase stishovite has been identified in the paired sample NWA 11522, this sample may have experienced higher shock pressures than NWA 7034 (Daly et al., 2018).

The majority of the ~6000 ppm water in the bulk sample of NWA 7034 may be located in hydrous Fe-oxide phases and phyllosilicates, with apatite contributing a maximum of 150 ± 50 ppm bulk water (Muttik et al., 2014). However, hydrous Fe-oxides and phyllosilicates are secondary alteration minerals unlike the apatites in NWA 7034, which are primary igneous minerals (McCubbin et al., 2016a). With the general formula $Ca_5(PO_4)_3(F,Cl,OH)$, apatite can accommodate varying amounts of water in its crystal structure. Although the apatites in NWA 7034 were reset at ~1.5 Ga and likely underwent exchange of F, Cl, and OH (McCubbin et al., 2016a; Barnes et al., 2020), some of this water may originate from the martian interior. Apatite occurs in all four clastic igneous lithologies recognized in NWA 7034: basalt, basaltic andesite, trachyandesite, and an Fe-, Ti-, and P-rich (FTP) lithology (Santos et al., 2015). Apatite differs between the clasts, with varying size, morphology, and abundance providing the opportunity to compare the H-isotopic compositions and water contents of different lithologies within the breccia, two of which (trachyandesite and FTP clasts) were previously unsampled in martian meteorites (Santos et al., 2015).

Measurements of melt inclusion glass and apatite in the least shocked martian meteorites (such as Nakhla; <20 GPa) indicate that the H-isotopic composition (reported as δD, defined as the D/H ratio relative to the terrestrial standard in parts per mil) of Mars' mantle is <275 ‰ (Hallis et al., 2012; Usui et al., 2012). This contrasts significantly with the martian atmosphere, which is isotopically heavy with a typical δD of ~6000 ‰ (Webster et al., 2013; Villanueva et al., 2015). Mars is thought to have lacked plate tectonics for much (if not all) of its geologic history, and so these two H-bearing reservoirs (the mantle and the atmosphere) are unlikely to have exchanged significantly. More recently, based on the analysis of glasses in three shergottites, a third significant hydrogen reservoir with an intermediate isotopic composition (δD = 1000–2000 ‰) has been proposed to exist in the martian crust (Usui et al., 2015); this is further supported by the work of Barnes et al. (2020). As NWA 7034 most closely represents the composition of the bulk crustal material on Mars, and it is the most water-rich of all known martian meteorites, its H-isotopic composition and water budget may more accurately reflect that of the martian crust than the other known meteorites and could provide a way to test the validity of this third reservoir (e.g., Barnes et al., 2020).

In this study, our goals are to: (1) constrain the H-isotopic composition of the apatite in various clasts and matrix of NWA 7034, (2) determine whether this mineral exhibits evidence for magmatic degassing or significant exchange with either the martian atmosphere or crustal fluids (i.e., whether the H-isotopic compositions of apatite are primary and represent the composition of the source mantle or whether they represent secondary processing, either in the mantle or crust), and (3) test the hypothesis of the presence of a third significant H-bearing reservoir on Mars in addition to the mantle and atmosphere.

2. Materials and Methods

2.1 Sample preparation

Chips of mineral standards (Table A1) were mounted in acrylic and anhydrously polished in multiple stages down to 0.5 μm grit size until they were suitable for secondary ion mass spectrometer (SIMS) analysis. After polishing, acrylic was removed and the mineral chips were cleaned using a sequence of ultrasonic baths modified after Aubaud et al. (2007): three 20 minute baths in acetone followed by three 20 minute baths in methanol. The mineral chips were then baked for a day at ~50ºC. Two pieces of NWA 7034 were cut from a larger slice of a whole stone (Fig. A1) and were polished anhydrously prior to co-mounting with standards in the same mounts in indium metal in separate one-inch aluminum discs (indium mounts; IM1 and IM2). We prepared dry, epoxy-free samples to ensure that the H-isotopic compositions and water contents of apatite were not modified during sample preparation. A slice of sample from the same piece of NWA 7034 mounted in IM1 was made into an epoxy mount (EM) using standard hydrous polishing methods; a discussion of the effects of preparing samples via traditional techniques (polished in the presence of water and mounted in epoxy) is presented in Appendix A. All mounts were then C-coated to a thickness suitable for electron microprobe and SIMS analysis.

2.2 Mineralogy and petrology analyses

Backscattered electron (BSE) images and X-ray element maps were obtained (operating conditions: 15 kV and 40 nA, 10 μm beam size, and 15 ms dwell time) with the Cameca SX-100 electron probe microanalyzer (EPMA) at the University of Arizona's Lunar and Planetary Laboratory (LPL). Element maps (F, Na, Mg, Al, Si, P, S, Cl, K, Ca, Ti, Cr, Mn, Fe, Zr) were used, in various combinations, to identify mineral phases for study (e.g., combined P-Mg-Al maps show the locations of apatite, pyroxene, and feldspar minerals). High resolution images of phases identified for quantitative analysis were obtained on the JEOL JXA-8530F field emission EPMA (operating conditions: 20 kV and 15 nA) at the Eyring Materials Center at Arizona State University (ASU). This instrument was also used to image the SIMS beam spots after isotopic analysis to ensure measurements were not compromised by underlying phases or cracks. Quantitative compositional analyses of major and minor element abundances in apatites (F, Na, Mg, Al, Si, P, S, Cl, Ca, Mn, Fe, La, Ce) were performed on the Cameca SX-100 at LPL with a beam current of 10 nA, a defocused beam, and counting times of 20 s on the peak and 10 s on each background for a total of 40 s per element. All data were reduced using a standard ZAF correction, Cl and F concentrations were corrected and the OH component was estimated using the method of Ketcham (2015) (Table A2; data were processed using the "approach 1" template in Ketcham, 2015). Detection limits were between 0.02 and 0.08 wt.%, with the exception of La (0.18 wt.%) and F (0.26 wt.%).

2.3 Isotopic analyses and determination of water content

Secondary ion mass spectrometer (SIMS) measurements of H-isotopic compositions and H_2O concentrations were performed on the Cameca IMS-6f at ASU using analytical protocols similar to those described in Mane et al. (2016) and Stephant et al. (2018). The instrument was baked prior to each analytical session to improve the vacuum and reduce the inherent H background; during runs the analysis chamber vacuum was kept at ~6–10 × 10^{-10} Torr. An electron gun was employed to maintain charge balance; prior to analysis, electron gun alignment was performed following the method of Chen et al. (2013) on the cathodoluminescent mineral benitoite that was co-mounted with the NWA 7034 thick sections and standards. Measurements were undertaken with a Cs^+ primary beam (~10 nA) that was rastered over a ~40 × 40 μm^2 area. A field aperture was used to limit the analyzed area to a circular 15 μm diameter area centered on the rastered region, reducing background H counts associated with crater edges. Each measurement consisted of 50 consecutive cycles each of H^- and D^- with counting times of 1 s and 10 s, respectively. The $^{16}O^-$ peak was measured at the end of each measurement to calculate the H/O ion ratio used for determination of H_2O content. The H_2O concentrations were estimated via a $H^-/^{16}O^-$ vs. H_2O calibration curve that included data for Durango apatite, the pyroxenes PMR 53 and the dehydrated "dry PMR 53", basaltic glass P-1326, and rhyolitic glass Macusani (Table A1). Water content calibrations were performed via the method of Mosenfelder et al. (2011), described as follows. The amount of H_2O background contamination was determined on the nominally anhydrous San Carlos olivine and dry PMR 53 pyroxene; at least three analyses of anhydrous phases were performed at the start of each analytical session and then monitored throughout the session. The average background value was subtracted from all standards and unknown phases analyzed in this study; the calibration curve was corrected for this H_2O background and forced through the origin. The H_2O

background was estimated to be ~58 ppm and ~67 ppm for IM1 and IM2 samples (indium-mounted, anhydrously-prepared), respectively. Since the EM (epoxy-mounted) sample was not co-mounted with standards, it was not possible to estimate the background in this manner; instead a background of approximately 127 ppm was estimated via analysis of anhydrous phases in this sample assuming that the H^-/O^- calibration remained consistent between mounts (see Appendix A). These backgrounds, similar to those reported during studies of lunar apatite (Tartèse et al., 2014) and Tissint merrilites (Stephant et al., 2018), are higher than often reported in SIMS analyses of H_2O concentrations employing small chips of material pressed into indium (e.g., Saal et al., 2008, 2013). The higher H background most likely results from the nature of the samples in this study; the thick sections of NWA 7034 have much larger surface areas and thicknesses than single grains/polished fragments employed in other studies and likely contain cracks and fractures that do not completely degas prior to sample analysis. NWA 7034 is also known to have the highest bulk water content of any martian meteorite (~6000 ppm; Agee et al., 2013), creating a potentially higher background than in studies of other (drier) samples as NWA 7034 acts as a "virtual leak." Based on repeated analyses of the Durango apatite standard throughout each analytical session, errors from counting statistics, and uncertainty in the instrumental background, we estimate the external reproducibility ($2\sigma_{SD}$) of the H_2O concentrations presented here to be ±20%, similar to Mane et al. (2016) and Stephant et al. (2018).

Hydrogen isotopic ratios (the ratio of ^2H or D to ^1H) are reported as deviations from Vienna Standard Mean Ocean Water (VSMOW) in per mil (‰), where VSMOW ($D/H_{VSMOW} = 155.76 \times 10^{-6}$) has a δD of 0 ‰ by definition, i.e., $\delta D = ([(D/H)_{sample}/(D/H)_{VSMOW}] - 1) \times 1000$. The δD values reported here are corrected for instrumental mass fractionation (IMF) and for the H-isotopic composition of instrumental background water. Durango apatite and the basaltic glass P-1326 were used to correct IMF and the isotopic composition of background water was determined on the nominally anhydrous so-called "dry PMR 53" pyroxene (a dehydrated form of the pyroxene PMR 53; Table A1). The δD value of the backgrounds, determined on the indium-mounted, anhydrously-prepared samples, were –120 ± 55 ‰ and –91 ± 88 ‰ during the two separate analytical sessions.

3. Results

3.1 Petrographic summary and elemental compositions of apatite

Apatite grains in multiple basalt and Fe-, Ti-, and P-rich (FTP) clasts, one impact melt clast, and interclastic matrix were analyzed in anhydrously-prepared slices of the martian polymict breccia NWA 7034 (Fig. 1, Table 1). No trachyandesite or basaltic andesite clasts were identified in this study. However, both those clast types are less common than basalt and FTP clasts. Moreover, basaltic andesite clasts may not contain apatite grains; those that do, have apatites that are <1 μm in diameter (Santos et al., 2015), below the spatial resolution of SIMS.

The largest apatite grains studied here were located in the interclastic matrix (up to ~190 μm diameter); apatite grains in FTP clasts were generally larger than in basaltic clasts (up to ~100 μm diameter vs. up to 40 μm diameter). All apatite studied here is Cl-rich

(Table A2), also known as chlorapatite, with higher Cl-contents than in most other martian meteorites (McCubbin et al., 2016b, 2016c). Although we did not observe any merrillite in this study, one instance of this phosphate mineral was previously identified in NWA 7034 as an inclusion in apatite (Liu et al., 2016).

3.2 Hydrogen isotopic compositions of apatite

Apatite grains in NWA 7034 show a range of δD values between 17 and 1164 ‰ (Table 1, Fig. 2). Apatite grains in the interclastic matrix (i.e., mineral fragments) and from the impact melt clast have the highest δD, on the order of ~1100 ‰. The apatite from an impact melt clast (Impact Melt A1, Grain 1; Table 1) has a heavy isotopic composition (δD = 1081 ± 18 ‰) and relatively low H_2O concentration (1173 ± 235 ppm) compared to other clastic apatite. There is no significant systematic difference between the isotopic compositions and H_2O concentrations of apatite grains from basalt clasts and FTP clasts (Fig. 2A). The FTP clasts contain a greater number of apatite grains with high H_2O concentrations compared to the basalt clasts, though this may be due to sampling bias as fewer apatite grains were analyzed in basalt clasts than in FTP clasts (8 vs. 14, respectively; Table 1). There is significant variability in the hydrogen isotope composition between apatite grains within the same clast (Fig. A2; Table 1). The H-isotopic compositions of the majority of NWA 7034 apatites (Fig. 2B) lie between those proposed for the martian mantle (δD of <275 ‰; Usui et al., 2012; Hallis et al., 2012) and a potential crustal reservoir (δD = 1000–2000 ‰; Usui et al., 2015) and overlap with those reported in previous studies (δD = 313–2459 ‰; Table 2; Fig. 3) (Hu et al., 2019; Barnes et al., 2020).

3.3 Water concentrations of apatite

The H_2O concentrations determined here via SIMS for NWA 7034 apatite range from 796 to 8201 ppm; the average H_2O concentration (3110 ± 1800 ppm; 2SD) agrees with the average values estimated via quantitative electron probe microanalysis (EPMA) data by Muttik et al. (2014; 3000 ± 1000 ppm). Water contents (reported as OH), and Cl and F concentrations, determined by stoichiometric difference in EPMA data (i.e., OH = 2–Cl–F for 10 Ca) were variable within individual apatite grains (Table A2), implying heterogeneous distribution of water in these grains. However, for many apatite grains, the method of Ketcham et al. (2015) yielded apparently negative OH contents. The likely explanation for this is that the EPMA data exhibit so-called F-acceleration, a well-known problem for EPMA measurements of apatite grains that leads to overestimation of F contents (e.g., Stormer et al., 1993). As such, F contents determined here are more likely overestimates and should be considered upper limits. As a result, we consider water concentrations determined directly via SIMS to be more accurate than those from stoichiometric difference via EPMA. Apparently negative OH values, determined via stoichiometric difference, have also been reported for apatite in other studies of NWA 7034 where SIMS data indicated the apatites were actually water-rich (e.g., Hu et al., 2019).

4. Discussion

4.1 Sources and effects of potential terrestrial contamination

There are two potential sources of terrestrial contamination in NWA 7034; hot desert weathering (this meteorite and its paired stones were found in Morocco) and sample preparation in the laboratory. Interior pieces of the NWA 7034 stone were used in this study to minimize the effects of terrestrial weathering. This alone cannot rule out all contamination and identifying and determining the extent of terrestrial weathering effects is not straight forward; since some martian meteorites exhibit only minor deviations in H-isotopic composition from terrestrial values, low δD is not necessarily indicative of terrestrial contamination (e.g., Hallis et al., 2012). Oxygen-isotope analysis of acid-washed and unwashed aliquots of NWA 7034 yielded similar isotopic values implying that there are few terrestrial alteration products present in this meteorite (Agee et al., 2013). However, H-isotope systematics may alter more readily than those of oxygen; timed hot desert-exposure of the severely shocked martian fall Tissint showed that even minor weathering on the scale of a few years can overprint the initial H-isotope systematics, increasing the water content and altering the isotopic composition (Stephant et al., 2018). Nevertheless, anhydrous phases like olivine were affected more than the phosphate merrillite, which appeared relatively unchanged after three years of desert-exposure. Realistically, the desert residence time of NWA 7034 is likely longer than a few years, possibly on the order of hundreds or thousands of years. Interclastic matrix would presumably alter more quickly than other material, as seen in chondrites (e.g., Schrader et al., 2014), but matrix apatite grains in NWA 7034 show no evidence for terrestrial alteration. In fact, they have some of the heaviest H-isotopic ratios and lowest H_2O concentrations, the opposite of what is expected if they were significantly terrestrially weathered. While terrestrial weathering of NWA 7034 during its residence in a hot desert cannot be completely ruled out, we anticipate that anhydrous phases would be more affected than those with higher water contents, such as apatite.

Anhydrous methods were used to reduce the potential for contamination during sample preparation and samples were stored in a dry nitrogen cabinet to minimize adsorbed water. A comparison with a sample prepared more traditionally with epoxy is included in Appendix A; apatite grains in the epoxy-mounted sample have slightly but systematically higher H_2O concentrations than those in the anhydrously prepared samples (858–10677 ppm vs. 796–8201 ppm H_2O, respectively) and have somewhat isotopically lighter H (δD = –69 to 961 ‰ vs. 17–1164 ‰, respectively) (Fig. A3). However, we cannot rule out the possibility that the minor differences in the measured H_2O concentrations and δD values between the epoxy-mounted and the anhydrously-prepared samples are simply a sampling artifact. Nevertheless, due to the inability to accurately correct for the abundance and isotopic composition of the instrumental H background for the apatite analyses conducted on the epoxy-mounted section of NWA 7034 (see discussion in Appendix A) we do not include those data in this discussion.

Although there is some overlap, the δD values (δD = 17–1164 ‰) determined here for apatite in NWA 7034 are lower, and H_2O concentrations (796–8201 ppm H_2O) are higher, than those estimated in two prior investigations conducted via NanoSIMS by Hu et al. (2019; δD = 313–2459 ‰; 184–3429 ppm H_2O) and Barnes et al. (2020; δD = 904–2030 ‰; 672–1728 ppm H_2O). A preliminary IMS-1280 SIMS investigation of NWA 11522 (Smith et al., 2019), a sample paired with NWA 7034, yielded δD values (δD = 52–782 ‰) and water concentrations (1380–5100 ppm H_2O) intermediate between those

reported here and those of the NanoSIMS studies of Hu et al. (2019) and Barnes et al. (2020). However, it is difficult to attribute the higher average water concentrations measured here to terrestrial contamination because our indium-mounted samples were prepared anhydrously.

Alternatively, these differences may be explained by inherent sample heterogeneities across the suite of regolith breccias. NWA 7533, another meteorite from the NWA 7034 pairing, has a bulk water content of ~8000 ppm (Beck et al., 2015), compared to ~6000 ppm determined for NWA 7034 (Agee et al., 2013); this indicates that these regolith breccias have highly variable water contents. It is possible that the NWA 7034 material studied here is inherently more H_2O-rich than the NWA 7034 samples analyzed in other studies.

Regardless of the care taken during sample preparation, it is also possible that traces of terrestrial water are still present within samples, and the extent to which this affects measured isotopic compositions depends on the analytical spatial resolution. For example, Hallis et al. (2012) suggested that their lower H-isotope ratios for Shergotty compared to another study (Greenwood et al., 2008) may have been due to their larger analysis spot size (8×8 μm^2 compared to 2×2 μm^2), with larger areas having higher potential for contribution from terrestrial contamination residing in micro-cracks. Other, older studies, with presumably larger spot sizes, showed lower or comparable values for Shergotty (Watson et al., 1994; Leshin, 2000; Boctor et al., 2003), but it is difficult to draw a definitive conclusion. Since OH appears to be heterogeneously distributed in apatite (Table A2; Hu et al., 2019), the larger effective analyzed areas of the IMS-6f SIMS (15 μm in diameter) and IMS-1280 SIMS (8 μm in diameter) compared to NanoSIMS (5 μm in diameter) would lead to the dilution of heavier isotopic compositions. Therefore, it is possible that the differences between studies result from a combination of inherent sample heterogeneities and differences between sample analysis techniques. Still, during the course of this study, care was taken to ensure that analyses were not compromised by cracks or fractures within apatite grains.

4.2 H-implantation during impact processing

The H-isotopic compositions of amphibole in martian meteorites appear to shift to isotopically heavier H and lower H_2O concentrations as a result of shock implantation of martian atmosphere and dehydration (see Hallis, 2017, and references therein). It is less apparent how the H-systematics of apatite are affected by shock processes. The NWA 7034 pairing group polymict breccias are the least-shocked martian meteorites (5–15 GPa; Wittmann et al., 2015), having experienced lower shock pressures than even the minimally shocked nakhlite Nakhla (<20 GPa; Greshake, 1998); this is evidenced by the lack of high-pressure minerals in NWA 7034. To test for the potential effects of impact processing, even at low shock pressure, apatite from an impact melt clast (assumed to have been formed during a breccia formation event in the petrogenetic history of NWA 7034) was analyzed; this apatite yields a δD value of 1081 ± 18 ‰ with H_2O concentration of 1173 ± 235 ppm (Table 1). While these results fit the trend for shock implantation and dehydration during impacts, such an interpretation should be considered with caution as it is based on only one data point. While it is possible that shock processes have affected the δD–H_2O systematics

in NWA 7034 apatites, this effect is likely most significant in impact melt clasts and relatively insignificant in igneous clasts as the co-existing feldspars in igneous clasts are plagioclase and not maskelynite (i.e., they have not experienced significant shock).

4.3 Fractional crystallization during magmatic degassing, crustal assimilation, or mixing with crustal water?

With the exception of the FTP clasts (the genesis of which remains enigmatic), all igneous lithologies (basalt, basaltic andesite, and trachyandesite clasts) in NWA 7034 exhibit apparent fractional crystallization behavior (Santos et al., 2015). Degassing of a magma can change its H-isotopic composition, and may occur via either dehydration (i.e., H_2O loss) or dehydrogenation (i.e., H_2 loss) depending on magmatic redox conditions. Dehydration typically leads to isotopically lighter δD in the magma (as the heavier hydrogen isotope is preferentially lost during H_2O loss) and a positive correlation between δD and H_2O concentrations. In contrast, dehydrogenation leads to isotopically heavier δD (as the lighter hydrogen isotope is preferentially lost during H_2 loss) and an inverse correlation between δD and H_2O concentrations (Demény et al., 2006), such as seen here for NWA 7034 apatites (Fig. 2A). This apparent dehydrogenation trend (increasing δD with decreasing water content) is also seen in apatite in other studies of NWA 7034 (Hu et al., 2019; Barnes et al., 2020), its paired sample NWA 11522 (Smith et al., 2019), shergottites (Watson et al., 1994; Boctor et al., 2003; Greenwood et al., 2008; Hallis et al., 2012; Hu et al., 2014), and ALH 84001 (Greenwood et al., 2008; Barnes et al., 2020) (Fig. 3), and in feldspathic glass in ALH 84001 (Boctor et al., 2003).

Under reducing conditions in lunar magmas, dehydrogenation can significantly increase δD in residual magmas; degassing of ~95–98% H_2 can increase δD by ~800–1000 ‰ and yields an inverse correlation between δD and H_2O content (e.g., Tartèse et al., 2013). For reduced shergottites, such as Tissint, H_2 degassing could explain some, but not all of the ~4000 ‰ variation in δD observed among the various phases; a significant fraction of this variation likely results from exchange with the isotopically heavy martian atmosphere (Mane et al., 2016). The ~1000 ‰ δD variation seen in NWA 7034 apatites here could be entirely attributed to dehydrogenation during magmatic degassing. However, high oxygen fugacities (fO_2), determined from magnetite-ilmenite pairs, have been reported for basalt (FMQ+2 to +4) and FTP clasts (FMQ–0.1 to FMQ+3). Under such oxidizing conditions, degassing is expected to occur via dehydration (i.e., H_2O loss) and would not result in the inverse relationship seen between H_2O concentrations and H-isotopic compositions. However, these oxidizing conditions may represent the fO_2 of secondary oxidation during subsolidus equilibration (Santos et al., 2015).

In mafic and felsic glasses of EETA 79001, ALH 84001, and ALH 77005 an inverse correlation between δD and H_2O concentrations was attributed to the addition of a low δD terrestrial contaminant to fractionated martian water (Boctor et al., 2003). However, while we cannot rule it out, we consider terrestrial contamination to be minimal in NWA 7034, particularly for apatite (see Section 4.1). Alternatively, the relationship seen in NWA 7034 apatites may be explained by crustal assimilation and/or mixing with fluids in a crustal reservoir. A similar δD–H_2O relationship seen in apatite from the QUE 94201 shergottite, which does not show evidence for crustal contamination (McCubbin et al., 2016b), was

attributed to the mixing between two martian reservoirs (Leshin, 2000). Whether the δD–H_2O systematics in NWA 7034 apatite record mixing or assimilation can be assessed by considering the F–Cl–OH X-site occupancy of apatite determined by quantitative EPMA (e.g., Table A2). Fractional crystallization pathways calculated by McCubbin et al. (2016b) show that, as crystallization progresses, apatite compositions become progressively more Cl-rich and subsequently more OH-rich. Whereas, if a magmatic system undergoes degassing during apatite crystallization, apatite compositions evolve toward F-rich compositions because F is more compatible in the melt; apatite compositions evolve to more Cl-rich compositions such as those seen in NWA 7034 during mixing or assimilation (McCubbin et al., 2016b). The dominance of Cl over F and OH in NWA 7034 apatites suggests that significant crustal assimilation or mixing with crustal fluid may have taken place (McCubbin et al., 2016b). Thus, the inverse relationship between H-isotopic composition and water content likely results from mixing of an original isotopically light (low δD) magmatic reservoir, such as seen in Nakhla (Hallis et al., 2012), with Cl-rich crustal fluid that was isotopically heavier (high δD) (Fig. 3). Isotopic exchange with this fluid appears to have been variable among the different apatite grains depending on their petrographic setting, with matrix apatites having undergone more exchange than clastic apatites, resulting in the generally higher δD seen in matrix apatites. The lower water content in the apatite grains with the heaviest δD could be achieved by the substitution of OH with Cl if the altering fluid had a low OH/Cl ratio. The timing of crustal fluid exchange likely coincides with the ~1.5 Ga reset age of the U-Pb systematics of zircons and apatites (McCubbin et al., 2016a; Barnes et al., 2020).

4.4 Primary magmatic signatures

Since there appears to have been significant post-eruption exchange of Cl and water in the crystal structure of NWA 7034 apatites, it is not appropriate to calculate the concentration of magmatic water in a coexisting melt at the time of apatite crystallization (McCubbin et al., 2016b; Smith et al., 2019). Nevertheless, the H-isotopic composition of the martian mantle may be reflected by a limited number of NWA 7034 apatite grains; H-isotopic compositions range from isotopically heavy (δD up to ~1100 ‰ for apatites in the impact melt clast and in the brecciated matrix) to isotopically light (δD ~0 ‰ in the apatite in the basaltic clast B2). The lightest δD value in the NWA 7034 apatite is similar to those in Nakhla apatites (δD = –78 to +188 ‰; Hallis et al., 2012), which were interpreted to be representative of the martian mantle. However, since NWA 7034 apatites have undergone significant post-crystallization alteration it is not possible to draw a definitive conclusion.

4.5 Water content and H-isotopic composition of the martian crust

Northwest Africa (NWA) 7034 and its paired samples chemically match the composition of the martian crust determined by spacecraft missions (Agee et al., 2013; Cannon et al., 2015). This is supported by a recent Cl isotope study of a suite of martian meteorites, which concluded that the Cl isotopic composition of the martian crust is defined by NWA 7034 with a $\delta^{37}Cl$ value of +1 ‰ (Williams et al., 2016).

The bulk rock water contents of NWA 7034 (6000 ppm H_2O; Agee et al., 2013) and NWA 7533 (~8000 ppm H_2O; Beck et al., 2015) indicate that these regolith breccias, which have basaltic bulk compositions, experienced significant addition of water following crystallization and brecciation of its source lithology. Indeed, a large fraction of the NWA 7034's bulk water is found in secondary alteration minerals, specifically hydrous Fe-oxides (hydromaghemite and an unidentified nanocrystalline Fe-bearing oxide phase) and phyllosilicates (saponite), with apatite accounting for only 150 ± 50 ppm of bulk H_2O (based on a 5% modal abundance of apatite; Muttik et al., 2014). Apatites in these regolith breccias appear to have undergone some degree of isotopic exchange with this crustal fluid during aqueous alteration; the majority of apatite grains appear to show mixing between two reservoirs, one of which was relatively isotopically heavy (Fig. 2A).

The heaviest H-isotopic compositions reported here for apatites in NWA 7034 (δD = ~1100 ‰) and those in the paired sample NWA 11522 (δD = ~780 ‰; Smith et al., 2019) are significantly lower than the heaviest δD values of apatites in ALH 84001 (δD up to ~3000 ‰) or the shergottites (δD up to ~4600 ‰) (Table 2; Fig. 3). Other studies of NWA 7034 apatites have found δD values up to ~2460 ‰ (Hu et al., 2019; Barnes et al., 2020), which are still significantly lower than those in apatites in all shergottites with the exception of Grove Mountains (GRV) 020090 (Hu et al., 2014) (Fig. 3). The heavier H-isotopic compositions of apatites in other martian meteorites have been attributed to one of the following: mixing of magmatic and surficial water (e.g., in ALH 84001; Boctor et al., 2003), mixing with near-surface water that has exchanged with the atmosphere (e.g., in the enriched shergottites; Greenwood et al., 2008), or they may represent a chemically heterogeneous mantle with multiple water reservoirs with different δD values (as suggested by Barnes et al., 2020). Based on analyses of quenched and impact glasses in three shergottites, Usui et al. (2015) proposed the existence of a globally extensive long-lived reservoir (either hydrated crust or ground ice interbedded between sediments). This reservoir is proposed to have a H-isotopic composition (δD = ~1000–2000 ‰) intermediate between an isotopically light mantle (δD = <275 ‰; Usui et al., 2012; Hallis et al., 2012) and the isotopically heavy present-day atmosphere (δD ~6000 ‰; Webster et al., 2013; Villanueva et al., 2015), and would have existed at least from the time the shergottites crystallized (~165–330 Ma; Nyquist et al., 2001) to when they were ejected by impacts (0.7–0.33 Ma), if not longer (Usui et al., 2015). The majority of the H-isotopic compositions of NWA 7034 apatites studied here (Fig. 2B) as well as the NWA 11522 apatites (from Smith et al., 2019) lie between those proposed for the martian mantle and the crustal reservoir suggested by Usui et al. (2015). The heaviest δD values in NWA 7034 apatites analyzed here are consistent with the lower limit on the δD value proposed for this intermediate reservoir; many of the apatite analyses from other studies of NWA 7034 fall within the proposed range for the martian crustal reservoir (Hu et al., 2019; Barnes et al., 2020), indicating that such a reservoir may indeed exist. Barnes et al. (2020) proposed a slightly wider range of H isotopic compositions for this crustal reservoir (δD ranging from ~750 to ~2250 ‰), which encompasses the H-isotopic compositions of apatites in both NWA 7034 and ALH 84001. Furthermore, our study supports the suggestion of Barnes et al. (2020) that such an intermediate crustal water reservoir likely persisted on Mars from more ancient times than the crystallization of the shergottites. Specifically, it is suggested that such a reservoir persisted from at least ~1.5 Ga (i.e., the timing of secondary alteration

of NWA 7034; McCubbin et al., 2016a; Cassata et al., 2018) and possibly from ~3.9 Ga (when ALH 84001 was subjected to hydrothermal alteration; Barnes et al., 2020).

The NWA 7034 zircon-bearing source lithologies have an old crystallization age (~4.4 Ga), pre-dating the formation of the shergottites (~165–330 Ma; Nyquist et al., 2001), when the martian atmosphere had a much lower δD (Hallis, 2017 and references therein). The timing of secondary alteration of NWA 7034 at ~1.5 Ga (McCubbin et al., 2016a; Cassata et al., 2018) also significantly predates shergottite formation. The majority of the δD values reported here for NWA 7034 apatites (up to ~1100 ‰) and in other studies (up to ~2460 ‰; Hu et al., 2019; Barnes et al., 2020), and for NWA 11522 apatites (up to ~780 ‰; Smith et al., 2019), are lower than those of quenched and impact glasses in three shergottites used by Usui et al. (2015) to infer the isotopic composition of the martian crust (δD = ~1000–2000 ‰). If one assumes that these differences are the result of interaction with crustal fluids of different compositions, then there are two potential explanations for isotopically lighter crustal fluids that may have altered NWA 7034 and the isotopically heavier ones that may have partially exchanged with enriched shergottites: (1) There could be multiple water-bearing reservoirs in the martian crust; a more prevalent (global and relatively long-lived) reservoir similar to that proposed by Usui et al. (2015), and recently also supported by Barnes et al. (2020), that is represented by NWA 7034 and ALH 84001 and more isolated (isotopically heavier) reservoirs recorded by the enriched and depleted shergottites, or (2) the H-isotopic compositions of NWA 7034 apatites represent an earlier stage in Mars' crustal evolution when altering fluids were more abundant and isotopically lighter (because they exchanged with an isotopically lighter atmosphere), while the enriched shergottites represent a later stage in martian crustal evolution when crustal fluids were isotopically heavier (likely from exchange with an evolved, isotopically heavier atmosphere). Alternatively, as suggested by Barnes et al. (2020), NWA 7034 and ALH 84001 may best represent the H-isotope composition of the global martian crustal reservoir proposed by Usui et al. (2015), while the heavy H-isotopic compositions seen in apatites from shergottites may represent chemical heterogeneities in the martian mantle and cannot be entirely attributed to shock-implanted atmospheric hydrogen as previously suggested.

5. Conclusion

In this study, we determined the water contents and H-isotopic compositions of apatite grains from a variety of lithological settings in the martian regolith breccia NWA 7034, including basaltic clasts, FTP clasts, impact melt clasts, and interclastic matrix. These apatite grains record a complex history of magmatic and impact processes, and exchange with crustal fluids. While the isotopically lightest apatite in NWA 7034 may reflect the composition of the martian mantle, or its close approximation, the variability in the majority of apatite H-isotopic compositions likely results from a combination of magmatic degassing and partial exchange with crustal water (which probably exchanged to some extent with the martian atmosphere) during a metamorphic event ~1.5 Ga. Since NWA 7034 so closely matches the chemical composition of much of the martian crust, these H-isotopic compositions are more representative of the martian crust than any other martian meteorite. Our study provides support for a crustal water reservoir with intermediate hydrogen isotope composition between that of the martian mantle and the

current martian atmosphere (δD = ~1000–2000 ‰) that likely persisted on Mars from at least ~1.5 Ga until the ejection time of NWA 7034 and the shergottites.

Acknowledgements

The authors thank Ken Domanik for assistance with the Cameca SX-100 EPMA at the University of Arizona, and Axel Wittmann for assistance with the JEOL JXA-8530F EPMA and Lynda Williams for assistance with the Cameca IMS-6f SIMS, both at Arizona State University. We are grateful to Laurence Garvie for assistance with sample preparation of the NWA 7034 samples. This manuscript was significantly improved by comments from two anonymous reviewers and the editorial expertise of R. Dasgupta. We acknowledge the use of facilities within the Eyring Materials Center at Arizona State University supported in part by NNCI-ECCS-1542160. We acknowledge NSF EAR 1352996 for support of the ASU SIMS facility.

Funding: This work was supported by the NASA Solar System Workings grant NNX16AT37G to M.W.

Davidson J., Wadhwa M., Hervig R., and Stephant A. (2020) Water on Mars: Insights from apatite in regolith breccia Northwest Africa 7034. *Earth and Planetary Science Letters* **552**, 116597.

583 **References**

584 C. B. Agee, N. V. Wilson, F. M. McCubbin, K. Ziegler, V. J. Polyak, Z. D. Sharp, Y.
585 Asmerom, M. H. Nunn, R. Shaheen, M. H. Thiemens, A. Steele, M. L. Fogel, R.
586 Bowden, M. Glamoclija, Z. Zhang, S. M. Elardo, 2013. Unique meteorite from early
587 Amazonian Mars: Water-rich basaltic breccia Northwest Africa 7034. *Science* **339**,
588 780–785.

589 C. Aubaud, A. C. Withers, M. Hirschmann, Y. Guan, L. A. Leshin, S. Mackwell, D. R.
590 Bell, 2007. Intercalibration of FTIR and SIMS for hydrogen measurements in glasses
591 and nominally anhydrous minerals. *Am. Mineral.* **92**, 811–828.

592 J. J. Barnes, F. M. McCubbin, A. R. Santos, J. M. D. Day, J. W. Boyce, S. P. Schwenzer,
593 U. Ott, I. A. Franchi, S. Messenger, M. Anand, and C. B. Agee, 2020. Multiple early-
594 formed water reservoirs in the interior of Mars. *Nature Geoscience* **13***,* 260–264.

595 P. Beck, A. Pommerol, B. Zanda, L. Remusat, J. P. Lorand, C. Göpel, R. Hewins, S. Pont,
596 E. Lewin, E. Quirico, B. Schmitt, G. Montes-Hernandez, A. Garenne, L. Bonal, O.
597 Proux, J. L. Hazemann, V. F. Chevrier, 2015. A Noachian source region for the "Black
598 Beauty" meteorite, and a source lithology for Mars surface hydrated dust? *Earth*
599 *Planet. Sci. Lett.* **427**, 104–111.

600 N. Z. Boctor, C. M. O'D. Alexander, J. Wang, E. Hauri, 2003. The sources of water in
601 Martian meteorites: clues from hydrogen isotopes. *Geochim. Cosmochim. Acta* **67**,
602 3971–3989.

603 G. A. Brennecka, L. E. Borg, M. Wadhwa, 2014. Insights into the Martian mantle: The age
604 and isotopics of the meteorite fall Tissint. *Meteorit. Planet. Sci.* **49**, 412–418.

605 K. M. Cannon, J. F. Mustard, C. B. Agee, 2015. Evidence for a widespread basaltic breccia
606 component in the martian low-albedo regions from the reflectance spectrum of
607 Northwest Africa 7034. *Icarus* **252**, 150–153.

608 W. M. Cassata, B. E. Cohen, D. F. Mark, R. Trappitsch, C. A. Crow, J. Wimpenny, M. R.
609 Lee, C. L. Smith, 2018. Chronology of martian breccia NWA 7034 and the formation
610 of the martian crustal dichotomy. *Sci. Adv.* **4**, eaap8306.

611 J. Chen, S. Schauer, R. Hervig, 2013. Normal-incidence Electron Gun alignment method
612 for negative ion analysis on insulators by magnetic sector SIMS. *Nucl. Instrum. Meth.*
613 *B.* **295**, 50–54.

614 L. Daly, M. R. Lee, B. E. Cohen, J. Cairney, K. Eder, L. Yang, M. A. Cox, A. J. Cavosie,
615 2018. High pressure excursions in the matrix of martian meteorite North West Africa
616 (NWA) 11522. *81st Annual Meeting of the Meteoritical Society,* #6237 (abs.).

617 A. Demény, T. W. Vennemann, S. Harangi, Z. Homonnay, I. Fórizs, 2006. H_2O– δD–Fe^{III}
618 relations of dehydrogenation and dehydration processes in magmatic amphiboles.
619 *Rapid Commun. Mass Spectrom.* **20**, 919–925.

620 J. Fritz, N. Artemieva, A. Greshake, 2005. Ejection of Martian meteorites. *Meteorit.*
621 *Planet. Sci.* **40**, 1393–1411.

Davidson J., Wadhwa M., Hervig R., and Stephant A. (2020) Water on Mars: Insights from apatite in regolith breccia Northwest Africa 7034. *Earth and Planetary Science Letters* **552**, 116597.

J. P. Greenwood, S. Itoh, N. Sakamoto, E. P. Vicenzi, H. Yurimoto, 2008. Hydrogen isotope evidence for loss of water from Mars through time. *Geophys. Res. Lett.* **35**, L05203.

A. Greshake, 1998. Transmission electron microscopy characterization of shock defects in minerals from the Nakhla SNC meteorite (abs). *Meteorit. Planet. Sci.* **33**, A63.

L. J. Hallis, 2017. D/H ratios of the inner Solar System. *Phil. Trans. R. Soc. A* **375**, 20150390.

L. J. Hallis, G. J. Taylor, K. Nagashima, G. R. Huss, 2012. Magmatic water in the martian meteorite Nakhla. *Earth Planet. Sci. Lett.* **359–360**, 84–92.

S. Hu, Y. Lin, J. Zhang, J. Hao, L. Feng, L. Xu, W. Yang, J. Yang, 2014. NanoSIMS analyses of apatite and melt inclusions in the GRV 020090 Martian meteorite: hydrogen isotope evidence for recent past underground hydrothermal activity on Mars. *Geochim. Cosmochim. Acta* **140**, 321–333.

S. Hu, Y. Lin, J. Zhang, J. Hao, W. Xing, T. Zhang, W. Yang, and H. Changela, 2019. Ancient geologic events on Mars revealed by zircons and apatites from the Martian regolith breccia NWA 7034. *Met. Planet. Sci*. DOI: 10.1111/maps.13256.

M. Humayun, A. Nemchin, B. Zanda, R. H. Hewins, M. Grange, A. Kennedy, J.-P. Lorand, C. Göpel, C. Fieni, S. Pont, D. Deldicque, 2013. Origin and age of the earliest Martian crust from meteorite NWA 7533. *Nature* **503**, 513–516.

R. A. Ketcham, 2015. Technical Note: Calculation of stoichiometry from EMP data for apatite and other phases with mixing on monovalent anion sites. *Am. Mineral.* **100**, 1620–1623.

T. J. Lapen, M. Righter, A. D. Brandon, V. Debaille, B. L. Beard, J. T. Shafer, A. H. Peslier, 2010. A younger age for ALH84001 and its geochemical link to shergottite sources in Mars. *Science* **328**, 347–351.

L. A. Leshin, 2000. Insights into Martian water reservoirs from analyses of Martian meteorite QUE 94201. *Geophys. Res. Lett.* **27**, 2017–2020.

Y. Liu, C. Ma, J. R. Beckett, Y. Chen, Y. Guan, 2016. Rare-earth-element minerals in martian breccia meteorites NWA 7034 and 7533: Implications for fluid–rock interaction in the martian crust. *Earth Planet. Sci. Lett.* **451**, 251–262.

P. Mane, R. Hervig, M. Wadhwa, L. A. J. Garvie, J. B. Balta, H. Y. McSween Jr., 2016. Hydrogen isotopic composition of the Martian mantle inferred from the newest Martian meteorite fall, Tissint. *Meteorit. Planet. Sci.* **51**, 2073–2091.

F. M. McCubbin, J. W. Boyce, T. Novák-Szabó, A. R. Santos, R. Tartèse, N. Muttik, G. Domokos, J. Vazquez, L. P. Keller, D. E. Moser, D. J. Jerolmack, C. K. Shearer, A. Steele, S. M. Elardo, Z. Rahman, M. Anand, T. Delhaye, C. B. Agee, 2016a. Geologic history of Martian regolith breccia Northwest Africa 7034: Evidence for hydrothermal activity and lithologic diversity in the Martian crust. *J. Geophys. Res. Planets* **121**, 2120–2149.

F. M. McCubbin, J. W. Boyce, P. Srinivasan, A. R. Santos, S. M. Elardo, J. Filiberto, A. Steele, C. K. Shearer, 2016b. Heterogeneous distribution of H_2O in the Martian interior:

Implications for the abundance of H_2O in depleted and enriched mantle sources. *Meteorit. Planet. Sci.* **51**, 2036–2060.

F. M. McCubbin, J. J. Barnes, A. R. Santos, J. W. Boyce, M. Anand, I. A. Franchi, C. B. Agee, 2016c. Hydrogen isotopic composition of apatite in Northwest Africa 7034: A record of the "intermediate" H-isotopic reservoir in the Martian crust? *47th Lunar and Planetary Science Conference*, #1326 (abs.).

H. Y. Jr. McSween, G. J. Taylor, and M. B. Wyatt, 2009. Elemental composition of the Martian crust. *Science* **324**, 736–739.

J. L. Mosenfelder, M. Le Voyer, G. R. Rossman, Y. Guan, D. R. Bell, P. D. Asimow, J. M. Eiler, 2011. Analysis of hydrogen in olivine by SIMS: Evaluation of standards and protocol. *Am. Mineral.* **96**, 1725–1741.

N. Muttik, F. M. McCubbin, L. P. Keller, A. R. Santos, W. A. McCutcheon, P. P. Provencio, Z. Rahman, C. K. Shearer, J. W. Boyce, C. B. Agee, 2014. Inventory of H_2O in the ancient Martian regolith from Northwest Africa 7034: The important role of Fe oxides. *Geophys. Res. Lett.* **41**, 8235–8244.

L. E. Nyquist, D. D. Bogard, C.-Y. Shih, A. Greshake, D. Stöffler, O. Eugster, 2001. Ages and geologic histories of martian meteorites. In: Chronology and Evolution of Mars (Eds. R. Kallenbach, J. Geiss, W. K. Hartmann). Space Science Series of ISSI, vol. 12. Springer, Dordrecht. Pp. 105–164.

L. E. Nyquist, C.-Y. Shih, F. M. McCubbin, A. R. Santos, C. K. Shearer, Z. X. Peng, P. V. Burger, C. B. Agee, 2016. Rb-Sr and Sm-Nd isotopic and REE studies of igneous components in the bulk matrix domain of Martian breccia Northwest Africa 7034. *Meteorit. Planet. Sci.* **51**, 483–498.

A. E. Saal, E. H. Hauri, M. L. Cascio, J. A. Van Orman, M. C. Rutherford, R. F. Cooper, 2008. Volatile content of lunar volcanic glasses and the presence of water in the Moon's interior. *Nature* **454**, 192–195.

A. E. Saal, E. H. Hauri, J. A. Van Orman, M. C. Rutherford, 2013. Hydrogen isotopes in lunar volcanic glasses and melt inclusions reveal a carbonaceous chondrite heritage. *Science* **340**, 1317–1320.

A. R. Santos, C. B. Agee, F. M. McCubbin, C. K. Shearer, P. V. Burger, R. Tartèse, M. Anand, 2015. Petrology of igneous clasts in Northwest Africa 7034: Implications for the petrologic diversity of the martian crust. *Geochim. Cosmochim. Acta* **157**, 56–85.

D. L. Schrader, J. Davidson, R. C. Greenwood, I. A. Franchi, J. M. Gibson, 2014. A water-ice rich minor body from the early Solar System: The CR chondrite parent asteroid. *Earth Planet. Sci. Lett.* **407**, 48–60.

A. Smith, L. J. Hallis, K. Nagashima, G. R. Huss, 2019. Hydrogen isotope analyses of apatite in martian polymict breccia Northwest Africa 11522. *50th Lunar and Planetary Science Conference*, #1850 (abs.).

A. Stephant, L. A. J. Garvie, P. Mane, R. Hervig, M. Wadhwa, 2018. Terrestrial exposure of a fresh Martian meteorite causes rapid changes in hydrogen isotopes and water concentrations. *Sci. Rep.* **8**, 12385.

Davidson J., Wadhwa M., Hervig R., and Stephant A. (2020) Water on Mars: Insights from apatite in regolith breccia Northwest Africa 7034. *Earth and Planetary Science Letters* **552**, 116597.

J. C. Stormer Jr., M. L. Pierson, and R. C. Tacker, 1993.Variation of F and Cl X-ray intensity due to anisotropic diffusion in apatite during electron microprobe analysis. *American Mineralogist* **78**, 641–648.

R. Tartèse, M. Anand, K. H. Joy, I. A. Franchi, 2014. H and Cl isotope systematics of apatite in brecciated lunar meteorites Northwest Africa 4472, Northwest Africa 773, Sayh al Uhaymir 169, and Kalahari 009. *Meteorit. Planet. Sci.* **49**, 2266–2289.

T. Usui, C. M. O'D. Alexander, J. Wang, J. I. Simon, J. H. Jones, 2012. Origin of water and mantle–crust interactions on Mars inferred from hydrogen isotopes and volatile element abundances of olivine-hosted melt inclusions of primitive shergottites. *Earth Planet. Sci. Lett.* **357–358**, 119–129.

T. Usui, C. M. O'D. Alexander, J. Wang, J. I. Simon, J. H. Jones, 2015. Meteoritic evidence for a previously unrecognized hydrogen reservoir on Mars. *Earth. Planet. Sci. Lett.* **410**, 140–151.

G. L. Villanueva, M. J. Mumma, R. E. Novak, H. U. Käufl, P. Hartogh, T. Encrenaz, A. Tokunaga, A. Khayat, M. D. Smith, 2015. Strong water isotopic anomalies in the martian atmosphere: Probing current and ancient reservoirs. *Science* **348**, 218–221.

L. L. Watson, I. D. Hutcheon, S. Epstein, E. M. Stolper, 1994. Water on Mars: Clues from deuterium/hydrogen and water contents of hydrous phases in SNC meteorites. *Science* **265**, 86–90.

C. R. Webster, P. R. Mahaffy, G. J. Flesch, P. B. Niles, J. H. Jones, L. A. Leshin, S. K. Atreya, J. C. Stern, L. E. Christensen, T. Owen, H. Franz, R. O. Pepin, A. Steele, the MSL Science Team, 2013. Isotope ratios of H, C, and O in CO_2 and H_2O of the Martian atmosphere. *Science* **341**, 260–263.

J. T. Williams, C. K. Shearer, Z. D. Sharp, P. V. Burger, F. M. McCubbin, A. R. Santos, C. Agee, K. D. McKeegan, 2016. The chlorine isotopic composition of Martian meteorites 1: Chlorine isotope composition of Martian mantle and crustal reservoir and their interactions. *Meteorit. Planet. Sci.* **51**, 2092–2110.

A. Wittmann, R. L. Korotev, B. L. Jolliff, A. J. Irving, D. E. Moser, I. Barker, D. Rumble III, 2015. Petrography and composition of Martian regolith breccia meteorite Northwest Africa 7475. *Meteorit. Planet. Sci.* **50**, 326–352.

736 **Figures (Color online only)**

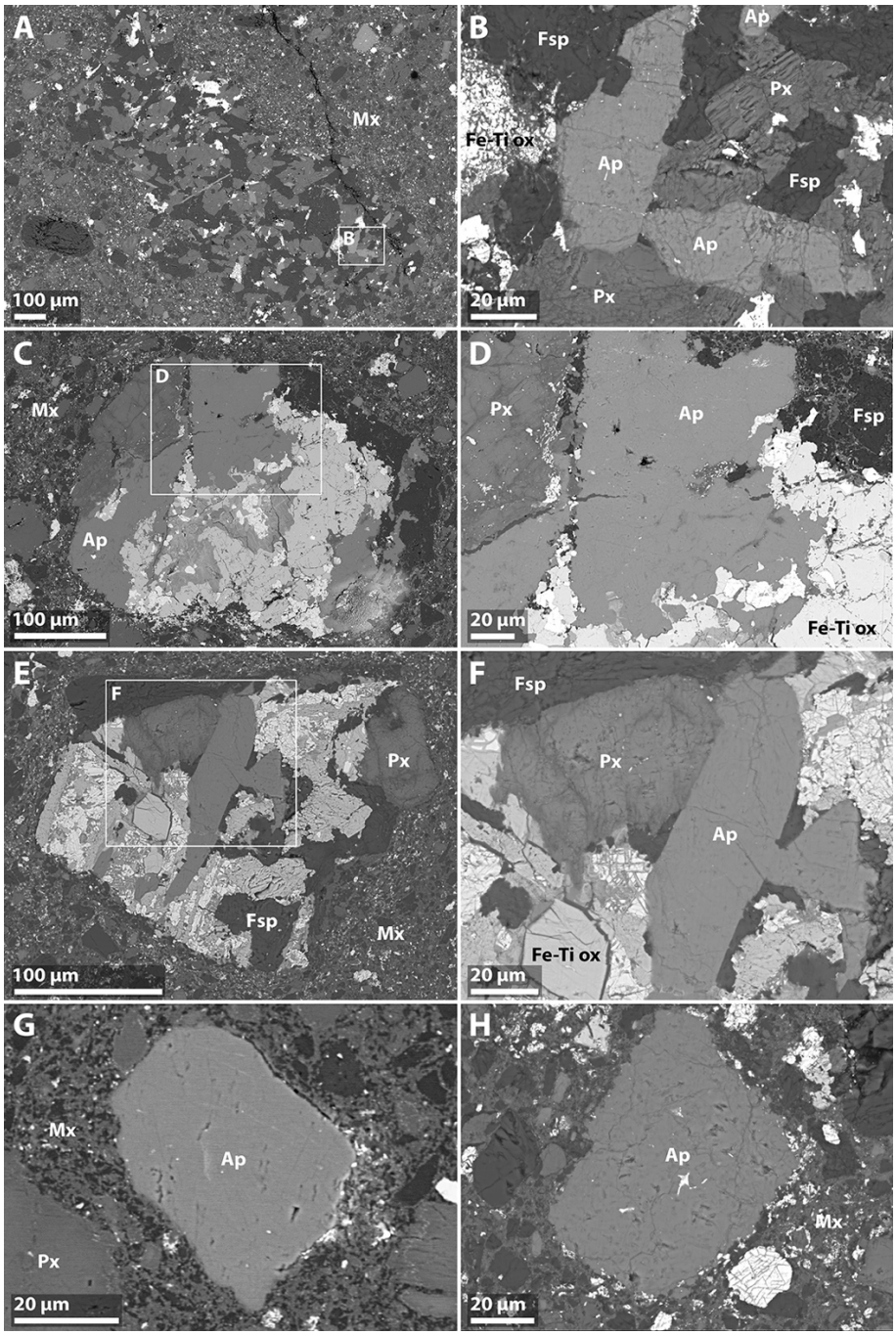

737

738 **Fig. 1.** Backscattered electron images of NWA 7034 apatite in; (**A,B**) a basaltic clast, (**C–**
739 **F**) FTP clasts, and (**G,H**) interclastic matrix. White boxes indicate the regions shown at
740 higher magnification images in adjacent panels. Ap = apatite, Fsp = feldspar, Fe-Ti ox =
741 Fe-Ti oxide, Mx = matrix, Px = pyroxene.
742

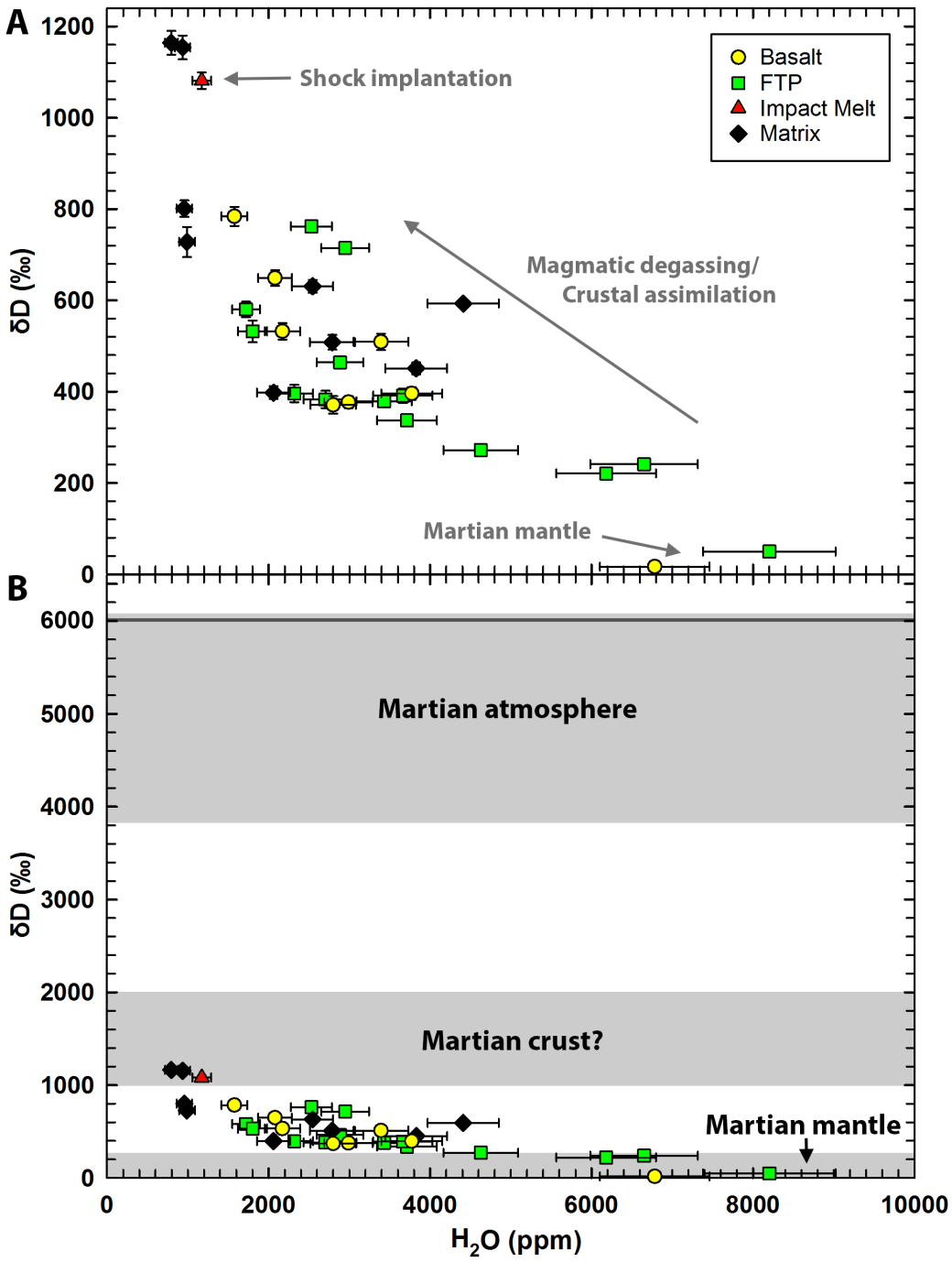

743

744 **Fig. 2.** H-isotopic composition versus water concentration in apatite from NWA 7034. (**A**)
745 Data from anhydrously-prepared samples grouped by lithological setting, either in various
746 clast types (basalt, FTP, and impact melt) or in interclastic matrix. (**B**) The same data are
747 shown along with fields representing the martian mantle (δD <275 ‰; Hallis et al., 2012;
748 Usui et al., 2012; Mane et al., 2016), intermediate crustal reservoir (δD = 1000–2000 ‰;
749 Usui et al., 2015), and the present-day atmosphere (δD = 4950 ± 1080 ‰; Webster et al.,
750 2013. Error bars represent 2σ uncertainties for δD (often smaller than the plotted symbols)

751 and, for the sake of clarity, 1σ uncertainties for H_2O concentrations. See Fig. A2 for a
752 similar plot for data on individual clasts.
753

754

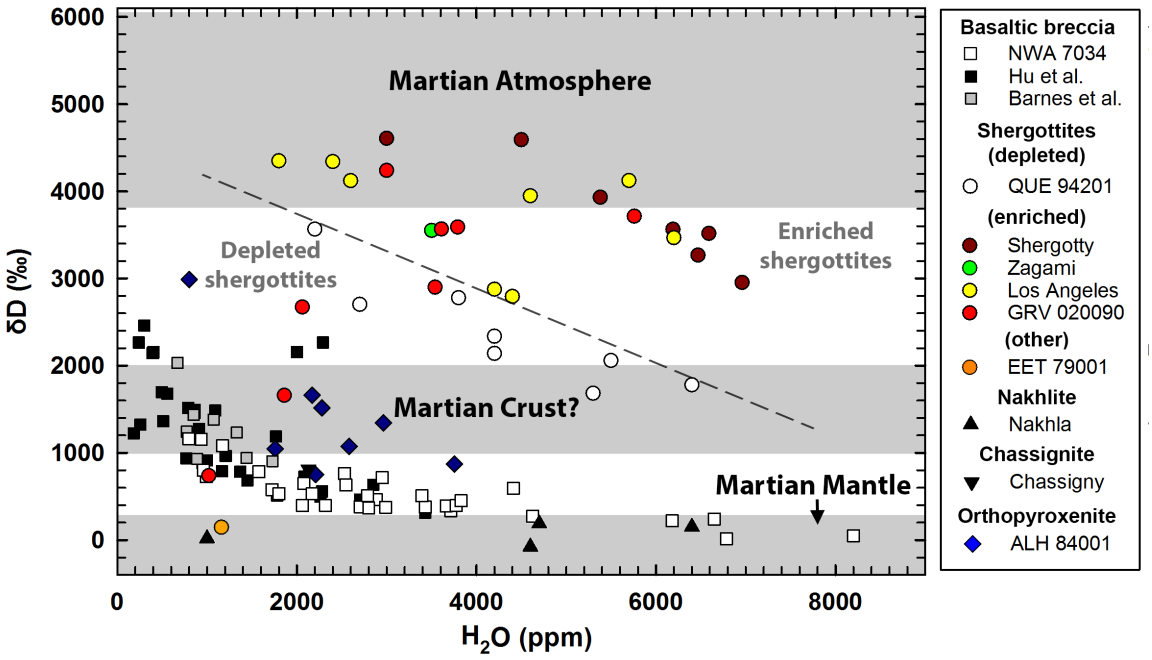

Fig. 3. H-isotopic composition versus water concentration in apatite from martian meteorites. Dotted line represents the approximate delineation of the dichotomy between enriched and depleted shergottites. Fields representing the mantle (<275 ‰; Hallis et al., 2012; Usui et al., 2012; Mane et al., 2016), intermediate crustal reservoir (δD = 1000–2000 ‰; Usui et al., 2015), and the present-day atmosphere (4950 ± 1080 ‰; Webster et al., 2013) are also shown. NWA 7034 data are from this study (open squares), Hu et al. (2019) (black squares), and Barnes et al. (2020) (gray squares); see Table 2 for data sources for other martian meteorites. For the sake of clarity, error bars are not shown.

765 **Tables**
766

Table 1. H-isotopic compositions (δD in ‰) and H_2O concentrations (ppm) of apatite grains in various clastic lithologies and interclastic matrix of NWA 7034. Errors (2σ) associated with water concentrations are estimated to be ±20%.

Clast/Matrix	Grain	δD (‰)	2σ	H_2O (ppm)	2σ
Basalt A1	31	509	18	3392	678
Basalt A1	32	649	17	2079	416
Basalt A1	33	377	13	2990	598
Basalt A1	35	784	21	1576	315
Basalt B1	6	396	14	3773	755
Basalt B2	3	532	18	2172	434
Basalt B2	4	17	10	6784	1357
Basalt B4	15	371	19	2800	560
FTP A3	10	337	10	3714	743
FTP A3	11	715	9	2949	590
FTP A3	12	379	13	3430	686
FTP A4	13	464	11	2884	577
FTP A4	14	50	7	8201	1640
FTP A5	4	383	19	2704	541
FTP A5	20	762	13	2530	506
FTP A6	27	580	17	1721	344
FTP A6	28	532	24	1801	360
FTP B3	12	396	19	2319	464
FTP B3	13	241	10	6651	1330
FTP B5	18	272	11	4627	925
FTP B6	21	391	16	3662	732
FTP B6	22	221	9	6181	1236
Impact Melt A1	1	1081	18	1173	235
Matrix A1	16	1154	26	935	187
Matrix A2	16b	1164	26	796	159
Matrix A3	22	398	14	2062	412
Matrix A4	78	728	33	990	198
Matrix B1	1	593	9	4410	882
Matrix B2	2	451	13	3827	765
Matrix B10	10	508	16	2788	558
Matrix B11	11	631	14	2545	509
Matrix B23	23	801	18	957	191

767
768

Table 2. Summary of H-isotopic compositions of apatites (determined via SIMS) in the martian meteorites.

	δD (‰)		H_2O (wt.%)		Crystallization age
Meteorite	**Min.**	**Max.**	**Min.**	**Max.**	**(Ma)**
Shergottite (depleted basaltic)					
QUE 94201	1683	3565	0.22	0.64	327 ± 10
Shergottite (enriched basaltic)					
Shergotty	2953	4606	0.30	0.70	165 ± 4
Zagami	2962	4358	~0.35		177 ± 3
Los Angeles	2794	4348	0.18	0.62	170 ± 8
GRV 020090	737	4239	0.10	0.58	
Shergottite (basaltic)					
EETA 79001	146		0.12		173 ± 3
Nakhlite (clinopyroxenite)					
Nakhla	–78	188	0.10	0.64	1270 ± 10
Chassignite (dunite)					
Chassigny	811		0.21		1340 ± 50
Orthopyroxenite					
ALH 84001	751	2988	0.08	0.38	4091 ± 30
Regolith breccia					
NWA 7034	313	2459	0.02	0.34	4420 ± 70
NWA 7034 (this study)	17	1164	0.08	0.82	

The hydrogen isotope and water concentration data for NWA 7034 apatites from this study only include analyses from the anhydrously-prepared samples. Literature sources of hydrogen isotope data for other martian meteorites are as follows: QUE 94201 (Leshin, 2000); Shergotty (Greenwood et al., 2008; Hallis et al., 2012), Zagami (Watson et al., 1994), Los Angeles (Greenwood et al., 2008), GRV 020090 (Hu et al., 2014), EETA 79001 (Boctor et al., 2003), Nakhla (Hallis et al., 2012), Chassigny (Boctor et al., 2003), ALH 84001 (Boctor et al., 2003; Greenwood et al., 2008; Barnes et al., 2020), and NWA 7034 (Hu et al., 2019; Barnes et al., 2020). Crystallization age data sources: QUE 94201 (Brennecka et al., 2014), Shergotty, Zagami, Los Angeles, EETA 79001, Nakhla and Chassigny (Nyquist et al., 2001), ALH 84001 (Lapen et al., 2010). The age provided here for NWA 7034 regolith breccia is the formation time of its source lithology (Cassata et al., 2018); it is noted that the timing of apatite resetting during thermal metamorphism due to hydrothermal activity is assumed to be at ~1500 Ma (McCubbin et al., 2016a).

769